

Short Communication

## Mn-doped LiFePO<sub>4</sub>/C Composite with Excellent High-Rate Performance as Lithium Ion Batteries Cathode

Shuning Zhao, Le Wen, Jinli Liu, JunQing Chen, Fengli Bei\*

China National Quality Supervision Testing Center for Industrial Explosive Materials, Nanjing University of Science and Technology, Nanjing, 210094, P.R. China

\*E-mail: [beifl@mail.njust.edu.cn](mailto:beifl@mail.njust.edu.cn)

Received: 12 May 2020 / Accepted: 9 July 2020 / Published: 10 August 2020

Nano-rod Mn-doped carbon coating LiFePO<sub>4</sub> composites have been synthesized by a simple solvothermal process coupled with calcination, which shows an excellent performance at high rate condition. The morphology and microstructure of the composites were evidenced by scanning electron microscopy (SEM), X-ray diffraction (XRD) and transmission electron microscopy (TEM). The electrochemical properties were evaluated by constant current charge/discharge test. Mn-doping magnified the interplanar spacing, providing a smoother aisle for ionic transport, it is beneficial to improve electrochemical properties at high rate. The stability was enhanced as well combined with carbon coating. In electrochemical measurement of the specific charge capacity, rate capacity and cycling stability, the obtained composite rod-like materials offer remarkably promising results for application, the initial discharge capacity is 160 mAh·g<sup>-1</sup> at 0.2 C and 120 mAh·g<sup>-1</sup> at 10 C, the capacity retention ratio is 94% at 0.2 C and 93% at 10 C after 50 charge-discharge cycles.

**Keywords:** LiFePO<sub>4</sub>, Manganese doping, high rate performance.

### 1. INTRODUCTION

Lithium ion battery(LIB) as a renewable energy source is a promising energy storage device for electric vehicles(EV),[1,2] however, it costs hours to get LIB fully charged, which limits the application, thus high rate performance is more and more important nowadays.[3-5] LiFePO<sub>4</sub> was originated as a lithium-ion cathode material in 1997, due to its element composition and structure, LiFePO<sub>4</sub> is superior in terms of thermal stability (350-500°C), high theoretical capacity(170 mAh·g<sup>-1</sup>),low cost, non-toxicity and high safety.[6-8] However, the crystal structure comprises of a network of FeO<sub>6</sub> octahedra and PO<sub>4</sub> tetrahedra, providing the only potential pathways for Li<sup>+</sup> diffusion in [010] directions, resulting in the intrinsic low lithium-ion migration rate (10<sup>-14</sup>-10<sup>-15</sup>cm<sup>2</sup>·S<sup>-1</sup>) and low electronic conductivity (10<sup>-9</sup>-10<sup>-10</sup> S·cm<sup>-1</sup>), this influenced high rate performance significantly, restricting the application of LiFePO<sub>4</sub>.[9,10]

Aiming at poor electrical conductivity of  $\text{LiFePO}_4$ , carbon coating is a widely used modification method.[11,12] Carbon materials including graphite, porous carbon, carbon nano tubes, graphene and so on are all attempted to make a combination with  $\text{LiFePO}_4$ . [13,14] These carbon materials can not only improve the conductivity of electrode materials to optimize the high rate performance, furthermore it can inhibit excessive growth and reunion of materials can be inhibited, which could reduce particle size during preparation.[15,16] For example, Wang utilized polyethylene glycol as carbon source and dopamine as nitrogen source to synthesize N-doped  $\text{LiFePO}_4/\text{C}$  composite by a novel spray drying method, which could adjust the thickness of coating. It can be observed that there is a thickness of 20nm amorphous N-C layer coated on the surface of the LFP. Results show that the synthesized 5%N-C@ $\text{LiFePO}_4$  has optimal performance with the of  $156\text{mAh}\cdot\text{g}^{-1}$  at a rate of 0.1C and  $121\text{mAh}\cdot\text{g}^{-1}$  at 5C, while the specific capacity of pure LFP is only  $90\text{mAh}\cdot\text{g}^{-1}$  at 5C. The capacity has a 30% increment at a high rate condition, which inform that the cooperation of N doping and C coating could sharply contribute to the high rate performance.[17]

Although carbon coating can enhance the overall conductivity of  $\text{LiFePO}_4$ , fundamentally, doping is an efficient method to improve material intrinsic conductivity.[18,19] The equivalent cation ( $\text{Mg}^{2+}$ ,  $\text{Cu}^{2+}$ ,  $\text{Co}^{2+}$ ) is more easily doped into the Fe position,  $\text{Ni}^{2+}$ ,  $\text{Co}^{2+}$ ,  $\text{Mn}^{2+}$  with  $0.069\text{\AA}$ ,  $0.065\text{\AA}$  and  $0.067\text{\AA}$  ionic radius doped into  $\text{Fe}^{2+}$  (ionic radius  $0.061\text{\AA}$ ) site could expand the lattice, closely packing of materials were not observed in microstructure so that enlarge  $\text{Li}^+$  diffusion channel and increase lithium ion diffusion coefficient, it could help to transfer  $\text{Li}^+$  more easier.[20,21] Jiang prepared different contents V-doped  $\text{LiFePO}_4/\text{C}$  composites (abbreviated as  $\text{LiFe}_{1-x}\text{V}_x\text{PO}_4@\text{C}$ ) through a facile sol-gel method followed by a thermal treatment. The sample are uniform with a particle size of 100 nm. Among all samples,  $\text{LiFe}_{0.97}\text{V}_{0.03}\text{PO}_4@\text{C}$  shows the best electrochemical performance and the discharge capacity is  $112.7\text{mAh}\cdot\text{g}^{-1}$  at 10 C after 200 cycles. The  $\text{LiFe}_{1-x}\text{V}_x\text{PO}_4@\text{C}$  electrodes exhibit superior rate performance and cycling stability for lithium-ion batteries compared with the undoped  $\text{LiFePO}_4@\text{C}$ , which confirms that V doping could further enhances high rate performance based on carbon coating.[22]

In this study, in order to improve the conductivity, the carbon coating and ion doping modification methods were applied together, we synthesized Mn doped carbon coating rod-like  $\text{LiFePO}_4$  by a sample solvothermal method coupled with subsequent calcination. During the solvothermal reaction process,  $\text{Mn}^{2+}$  doping was achieved by adding  $\text{MnSO}_4\cdot\text{H}_2\text{O}$ , glucose was added after that as a carbon resource. Combined with two modification methods, the composites are expected to exhibit superior performance in terms of the high rate capability and cyclic stability, and a promising excellent positive electrode material for high rate performance lithium-ion power batteries.

## 2. EXPERIMENTAL

### 2.1 Materials

$\text{LiFe}_{0.975}\text{Mn}_{0.025}\text{PO}_4/\text{C}$  composite materials were prepared by solvothermal method. The samples were synthesized by  $\text{LiOH}\cdot\text{H}_2\text{O}$  (AR),  $\text{H}_3\text{PO}_4$  (85%, AR),  $\text{FeSO}_4\cdot 7\text{H}_2\text{O}$  (AR),  $\text{MnSO}_4\cdot\text{H}_2\text{O}$  (AR), ethylene glycol (EG, AR), glucose( $\text{C}_{12}\text{H}_{22}\text{O}_{11}$ , AR) along with Ascorbic acid (AR) as reductive agent

and carbon source.

## 2.2 Synthesis of $\text{LiFe}_{0.975}\text{Mn}_{0.025}\text{PO}_4/\text{C}$

$\text{LiFe}_{0.975}\text{Mn}_{0.025}\text{PO}_4/\text{C}$  composite was prepared via a solvothermal route using  $\text{FeSO}_4 \cdot 7\text{H}_2\text{O} + \text{MnSO}_4 \cdot \text{H}_2\text{O}$ ,  $\text{H}_3\text{PO}_4$  and  $\text{LiOH} \cdot \text{H}_2\text{O}$  with the molar ratio of 1:1:3. Firstly, 0.6 M  $\text{LiOH}$  was dissolved in deionized water and then 0.2 M  $\text{H}_3\text{PO}_4$  was added dropwise, finally white precipitate was generated. Then 0.2 M  $\text{FeSO}_4 \cdot 7\text{H}_2\text{O} + \text{MnSO}_4 \cdot \text{H}_2\text{O}$  and moderate ascorbic acid was dissolved in a mass of EG, the mixture was added to the white precipitate dropwise and stirred vigorously for 15 min. Subsequently, the resulting mixture was then quickly transferred into a 100 mL Teflon-lined stainless steel autoclave followed by the heating at  $180^\circ\text{C}$  for 16 h. After cooling down to the room temperature, the precipitate was filtrated and washed with deionized water, which was then dried at  $70^\circ\text{C}$  for 6h. Next, the powder was annealed at  $500^\circ\text{C}$  for 5 h under the flowing nitrogen. The samples obtained in this manner are hereafter abbreviated as  $\text{LiFe}_{0.975}\text{Mn}_{0.025}\text{PO}_4$  (noted as LFMP), the pure  $\text{LiFePO}_4$  without Mn doping was prepared for comparison, noted as LFP. The precursor  $\text{LiFe}_{0.975}\text{Mn}_{0.025}\text{PO}_4$  was mixed with 5wt% glucose by mechanical lapping, then the powder was annealed at  $500^\circ\text{C}$  for 5h under the flowing nitrogen, the products were noted as LFMP-C, the pure  $\text{LiFePO}_4$  was coated by same method, noted as LFPC.

## 2.4 Characterization and electrochemical measurements

The crystalline phase of the samples were analyzed by powder X-ray diffraction (XRD, BRUKER D8) which was performed using  $\text{Cu K}\alpha$  radiation ( $\lambda = 1.54056 \text{ \AA}$ ). Data were collected from  $10^\circ$  to  $80^\circ$  in  $2\theta$ , with a step size of  $0.05^\circ$  at room temperature. The morphology and particle size of the prepared nanocrystals were monitored by a scanning electron microscopy (FEI SIRION200). The fine structures of prepared nanostructures were analyzed by a transmission electron microscopy (JEOL JEM-2100F).

A cathode working electrode for electrochemical testing was prepared by mixing product with acetylene black as conducting agent and polyvinylidene (PVDF) as binder in N-methylpyrrolidone (NMP) with weight ratio 80:10:10. Magnetic stir was continued until formed uniform slurry was formed. Then the mixed slurry was spread uniformly on a thin aluminum foil and subsequently dried at  $90^\circ\text{C}$  for 12 h under vacuum. Metal lithium foils were used as the counter electrodes. The electrolyte was 1M  $\text{LiPF}_6$  solution in a mixed solvent of ethylene carbonate (EC), dimethyl carbonate (DMC) and ethyl methyl carbonate (EMC) (EC:DMC:EMC=1:1:1, V/V). A polypropylene microporous film was used as the separator. The cells were assembled in an argon filled glove box. The modle number of cell is CR2016. The cells were charged and discharged at room temperature between 2.0 and 4.2 V versus  $\text{Li}^+/\text{Li}$  on the electrochemical test instrument (CT2001A, Wuhan Land Electronic Co. Ltd., China).

## 3. RESULTS AND DISCUSSION

As shown in Fig.1, the prepared four samples could all precisely corresponding to the  $\text{LiFePO}_4$

standard XRD card(PDF#40-1499) without impurities,[23,24] the sharp peaks show a excellent crystallinity. The XRD comparison of LFP and LFP/C shows that carbon coating makes no effect to the patterns, indicating that carbon coating did not change the olivine structure of LFP.

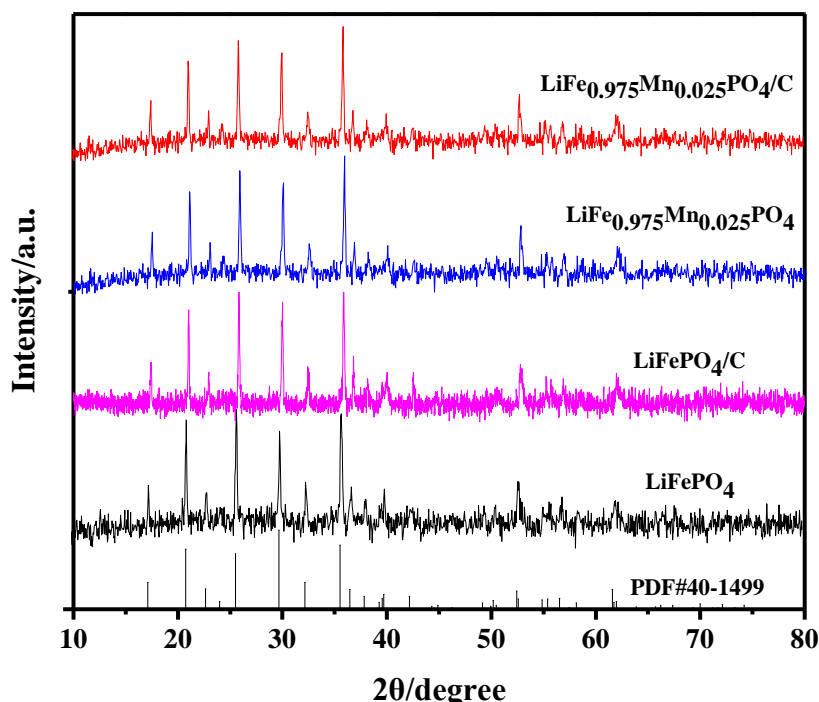


Figure 1. XRD patterns of LFP、LFP/C、LMFP、LMFP/C

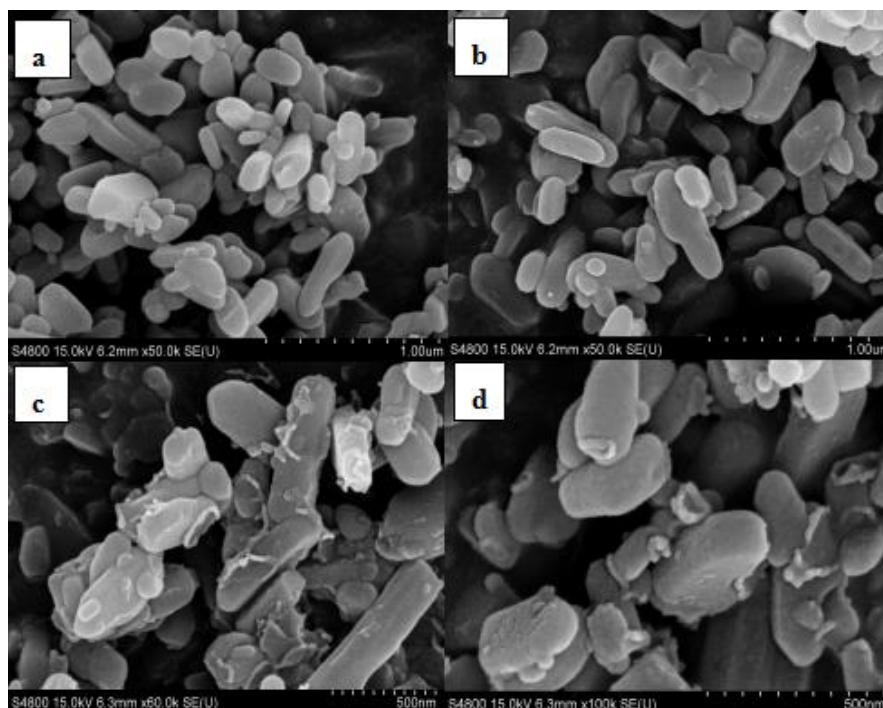
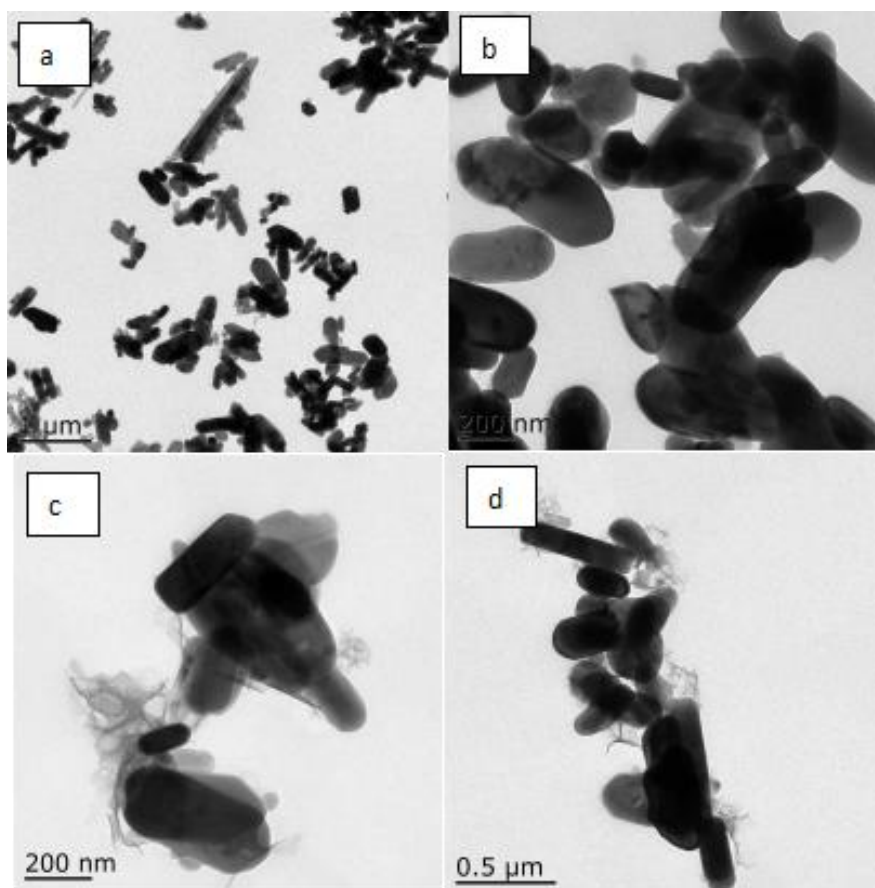


Figure 2. SEM images of LFP(a)、LMFP(b)、LFP/C(c)、LMFP/C(d)



**Figure 3.** TEM images of LFP(a)、LMFP(b)、LFP/C(c)、LMFP/C(d)

This can be attributed to the low proportion of coating materials in active materials. The peaks of the samples doped with manganese have a excursion to smaller angle, which proved the successful doping of manganese, similar phenomenon appeared in other Mn-doped  $\text{LiFePO}_4$  works.[25,26] Because of the larger radius of  $\text{Mn}^{2+}$ (0.97Å, while the radius of  $\text{Fe}^{2+}$  is 0.92Å), the crystal plane gap magnified, leading to smaller angles of peaks on the XRD patterns.[27] The increased layer spacing is benefit to rapid diffusion of  $\text{Li}^+$ , which could account for the enhanced high rate performance.

From SEM and TEM images (shown in Fig. 2(a) and Fig. 3(a)), it can be clearly observed that the pure  $\text{LiFePO}_4$  are rod-like morphology, the particles are quite uniform in partical size, typically in a narrow range of 200-600 nm. Negligible change in morphology s observed by comparison of Fig.2(a) and Fig.2(b), proving that the doping of  $\text{Mn}^{2+}$  does not influence on morphology, which is consistent with the XRD results, and the surface of rods are smooth. Seen, it is obviously noted from Fig.2(c) and Fig.3(c) that it adheres to LFP surface in the form of carbon deposition after calcining glucose. The quantity of the glucose addition is only the 5% percent of the yield of pure LFP, the content is too small to affect the whole morphology structure. Carbon deposition is not completely coated on the surface of the LFP while carbon coating on the whole surface will prevent the transfer of  $\text{Li}^+$ . During carbon deposition process, the morphology and particle size remained unchanged. In the meantime, the carbon deposition acts as barriers between particles, which reduced the agglomeration and prevented further particle growth,[28] so LFP/C has a better dispersion compared with pure LFP, which shows the same

results as other LFP/C materials.[29] At the same time, similar to other coatings, carbon coating can also maintain the stability of the material structure. The SEM and TEM images of LMFP/C are similar with LFP/C (Fig.2(c)(d), Fig. 3(c)(d)), which could prove the  $\text{Mn}^{2+}$  doping and C coating keep the intrinsic properties of LFP.

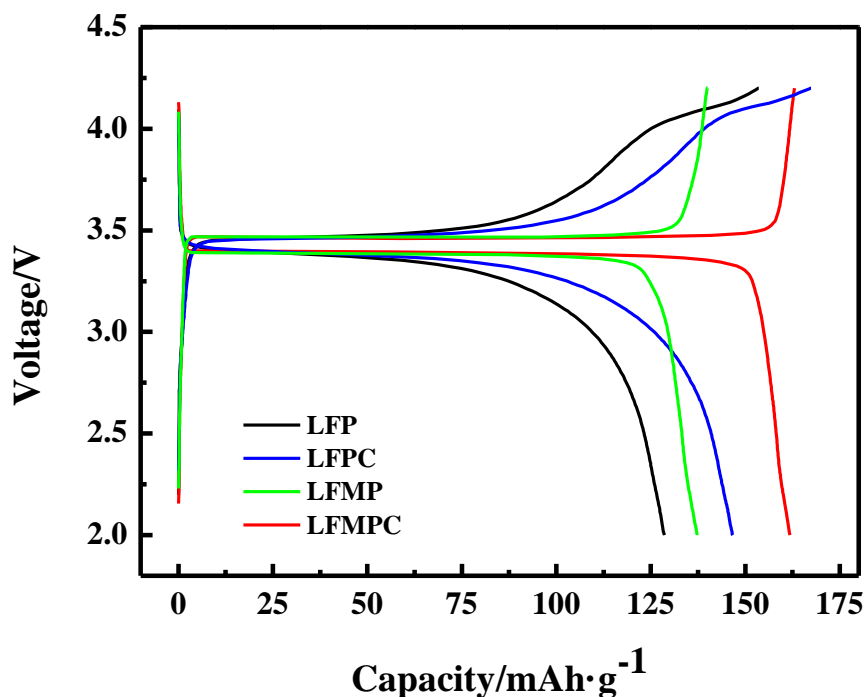


**Figure 4.** Initial charge/discharge curves of LFP,LFP/C, LFMP,LFMP/C at 0.2C

To enhance  $\text{LiFePO}_4$  electrochemical property, ion doping is a commonly used method. The purpose of ion doping is to enhance the electron conductivity and ion mobility of  $\text{LiFePO}_4$  material, some ion doping, such as  $\text{Mn}^{2+}$  doping could contribute to on material stability. Fig.4 compares the initial charge-discharge voltage profiles of LFP, LFPC, LMFP and LMFP/C electrode materials at 0.2 C rate at room temperature ( $25^\circ\text{C}$ ). It demonstrates that all the samples exhibit typical flat charge-discharge plateaus around 3.4 V, similar charge-discharge profiles have been observed in many LFP/C composites,[30,31] because of the little Mn content ,there is no change in voltage platform. It is obviously that Mn doped materials owe a flatter platform, and the capacities have a slight improvement (from  $128 \text{ mAh}\cdot\text{g}^{-1}$  to  $137 \text{ mAh}\cdot\text{g}^{-1}$ ). Because of ,  $\text{Mn}^{2+}$  could occupy the location of  $\text{Fe}^{2+}$  to increase the lattice constant of the material due to larger radius of  $\text{Mn}^{2+}$  than  $\text{Fe}^{2+}$ . The size of  $\text{Li}^+$  diffusion path is enlarged with the increased interplanar spacing, which makes the  $\text{Li}^+$  inserting and taking off more easier, thus leading to more  $\text{Li}^+$  participation in the charge/discharge process. On the other hand,  $\text{Mn}^{2+}$  doping could reduce polarization phenomenon, because smoother de-intercalation of  $\text{Li}^+$  could reduce concentration and resistance polarization.[32] From Fig.4, the charge and discharge voltage differences of LFP and LFMP are 0.38 V and 0.1 V, respectively when capacity reaches up to  $100 \text{ mAh}\cdot\text{g}^{-1}$ . To sum up, the effect of  $\text{Mn}^{2+}$  doping on the enhanced discharge specific capacity and the decreased polarization of  $\text{LiFePO}_4$  is significant. Carbon coating in a sense provides a role of pseudocapacitance, both LFP/C

and LFMP/C owing gentler downhill after the platform during the discharge process compared with LFP and LFMP, which could enable the discharge voltage drop slower in order to enhance the discharge voltage.

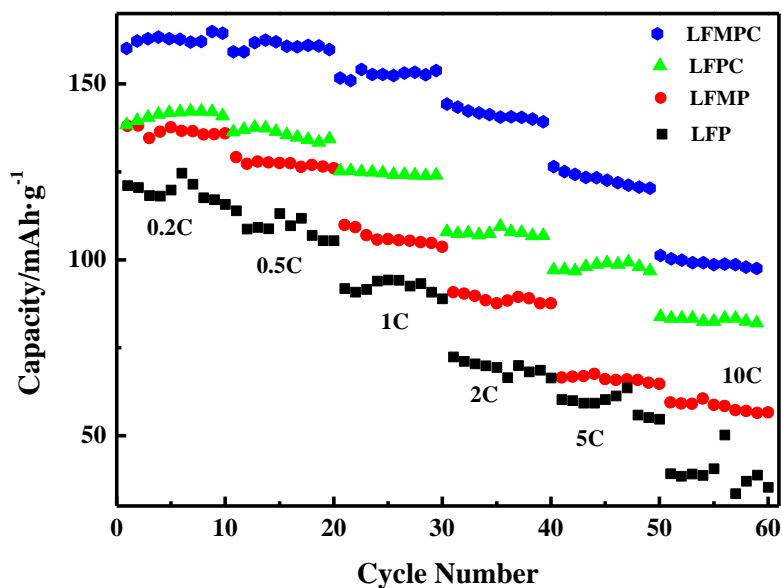


Figure 5. Cycle performance of LFP, LFP/C, LFMP and LFMP/C at different rates

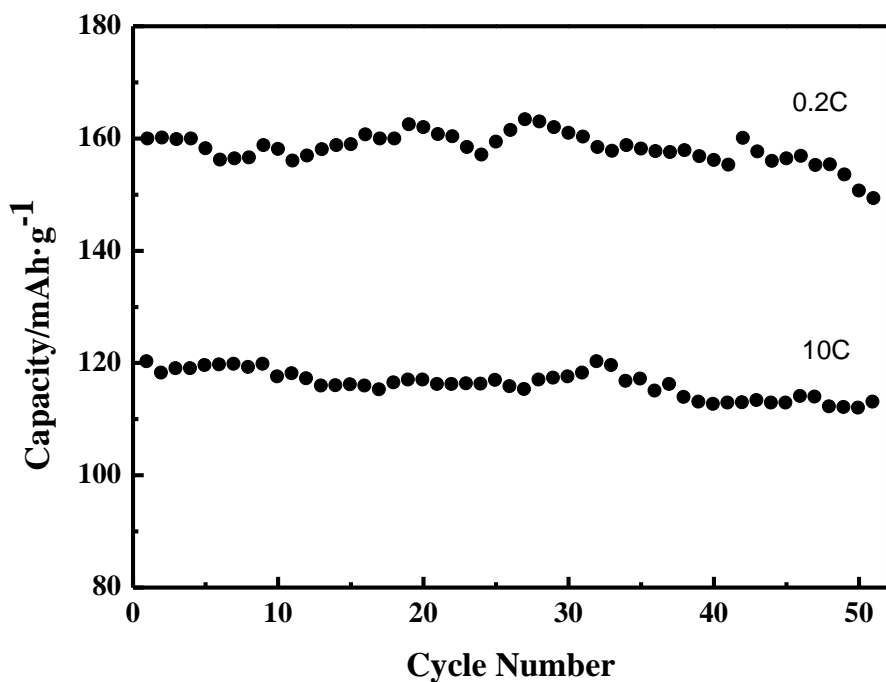


Figure 6. Cycle performance of LFMP/C at 0.2C and 10C

LiFePO<sub>4</sub> often shows a bad rate performance due to its low conductivity and ion mobility. In

addition to stabilizing the structure, carbon coating could increase the surface conductivity of  $\text{LiFePO}_4$ , thus the rate performance of LFP/C and LFMP/C is much better than LFP and LFMP, respectively. Fig.5 shows the discharge capacities of LFP, LFP/C, LFMP and LFMP/C at 0.2 C, 0.5 C, 1 C, 2 C, 5 C and 10 C, ten cycles for each rate, the initial discharge capacities are 120, 137, 138 and 160  $\text{mAh}\cdot\text{g}^{-1}$ , respectively, it implies a 30% increment of initial discharge capacity upon carbon coating and  $\text{Mn}^{2+}$  doping. As for rate performance, LFMP/C shows 120  $\text{mAh}\cdot\text{g}^{-1}$  discharge capacity at 10C, the capacity retention is 75%, while the pure LFP only has 35  $\text{mAh}\cdot\text{g}^{-1}$  capacity left, and the capacity retention is 29%. While it is not hard to reach a high discharge capacity at low rate, a sluggish slope appeared in most  $\text{LiFePO}_4/\text{C}$  materials when the rate come up. For example, at the rate of 0.5 C and 10 C, the capacities of LFMP/C (157 and 120  $\text{mAh}\cdot\text{g}^{-1}$ ) are higher than porous  $\text{LiFePO}_4/\text{C}$  nanocomposite (156.1 and 108.6  $\text{mAh}\cdot\text{g}^{-1}$ ) [33] and interconnected  $\text{LiFePO}_4/\text{C}$  microspheres (155.5 and 100.2  $\text{mAh}\cdot\text{g}^{-1}$ ). [34] Because  $\text{Mn}^{2+}$  doping could provide a larger aisle, and carbon coating could enhance the conductivity, the rate performance of  $\text{LiFePO}_4$  material improve evidently, which enabling  $\text{LiFePO}_4$  used more wildly and better prospects.

Cyclic stability especially at large rate is an important index of  $\text{LiFePO}_4$ . Fig.6 shows the cycle performance of LFMP/C at 0.2 C and 10 C after 50 charge-discharge cycles. When the rate is 0.2 C, the initial discharge is 160  $\text{mAh}\cdot\text{g}^{-1}$ , it is a delightful result because it is very close to the the theoretical capacity of  $\text{LiFePO}_4$  (170  $\text{mAh}\cdot\text{g}^{-1}$ ). After 50 charge-discharge cycles, the discharge capacity keeps 150 $\text{mAh}\cdot\text{g}^{-1}$ , the capacity retention is nearly 94%, which could illustrate that LFMP/C owns perfect cyclic stability. The initial discharge capacity is 120  $\text{mAh}\cdot\text{g}^{-1}$  at 10 C, maintaining 112 $\text{mAh}\cdot\text{g}^{-1}$  after 50 cycles, the capacity retention is 93%, it is more surprising that it still has perfect cyclic stability at large rate compared with the stability at small rate. The high specific capacity and cyclic stability of LFMP/C might originated from the more smooth aisle and better conductivity.

**Table 1.** Summary of various ion-doped  $\text{LiFePO}_4$  prepared by different methods and different carbon sources

Synthesis methods	Doping ion	Carbon source	specific capacity ( $\text{mAh}\cdot\text{g}^{-1}$ )
sol-gel[22]	$\text{V}^{5+}$	citric acid	117.4 $\text{mAh}\cdot\text{g}^{-1}$ (10C)
wet milling-spray drying-carbothermal reduction (WSC)[35]	$\text{V}^{3+}, \text{F}^-$	starch	136 $\text{mAh}\cdot\text{g}^{-1}$ (10C)
hydrothermal [36]	$\text{Mn}^{2+}$	$\text{C}_6\text{H}_{12}\text{O}_6\cdot\text{H}_2\text{O}$	110 $\text{mAh}\cdot\text{g}^{-1}$ (5C)
continuous composition spread (CCS)[37]	$\text{Mn}^{2+}$	None	140 $\text{mAh}\cdot\text{g}^{-1}$ (1C)
solvothermal (this study)	$\text{Mn}^{2+}$	glucose	120 $\text{mAh}\cdot\text{g}^{-1}$ (10C)

Table 1 illustrates the electrochemical performance of metal ion-doped  $\text{LiFePO}_4$  prepared by various methods from other laboratory in three years. A series of developments are achieved compared



with previous work. Firstly, our synthesis method is facile and green, the carbon source is cheap and the energy consumption is lower. Secondly, except for  $V^{3+}$ ,  $F^-$  co-doping material with a capacity of  $136 \text{ mAh}\cdot\text{g}^{-1}$  at 10C,[23] the electrochemical performance of our material is outstanding. While the third materials is more similar with this study,[36] because of small changes in detail, our material shows better performance, especially at high rate ( $120 \text{ mAh}\cdot\text{g}^{-1}$ (10C) vs.  $110 \text{ mAh}\cdot\text{g}^{-1}$ (5C)). Although carbon coating and ion-doping are common modification methods for  $\text{LiFePO}_4$  based on saving cost energy, the rate performance enhanced significantly compared with previous reports.

#### 4. CONCLUSIONS

In summary, a cheap and successful modification method for  $\text{LiFePO}_4$  using a simple solvothermal method coupled with high-temperature calcination was proposed. The  $\text{Mn}^{2+}$  doping could increase the lattice constant of  $\text{LiFePO}_4$  and improve the electrochemical accessibility, which makes it easier for  $\text{Li}^+$  inserting and taking off. The smoother aisle greatly promotes rate performance. Cooperating with carbon coating, the structure of  $\text{LiFePO}_4$  could not be easily damaged, it could also increase the conductivity. Therefore, modified LFP battery performances are increased compared with pure LFP, the initial discharge capacity is  $120 \text{ mAh}\cdot\text{g}^{-1}$  at 10 C, keeping  $112 \text{ mAh}\cdot\text{g}^{-1}$  after 50 cycles, the capacity retention is 93%, comparing to the stability at small rate, it is more surprising that it still exhibits perfect cyclic stability at large rate. The enhancement in high rate is most valuable among them, which reduces the restriction of LFP material and increase the application area.

#### ACKNOWLEDGEMENTS

This work was partially supported by the National Natural Science Foundation of China (51472119 and 21474053) and A Project Funded by the Priority Academic Program Development of Jiangsu Higher Education Institutions (PAPD). Thanks support from China National Quality Supervision Testing Center for Industrial Explosive Materials, Nanjing University of Science and Technology.

#### References

1. A. Tron, S. Jeong, Y.D. Park and J. Mun, *ACS Sustain. Chem. Eng.*, 7 (2019) 14531.
2. X.N. Feng, D.S. Ren, S.C. Zhang, X.M. He, L. Wang and M.G. Ouyang, *Int. J. Electrochem. Sci.*, 14 (2019) 44
3. Y.S. Meng, Y.Z. Li, J. Xia, Q.R. Hu, X.Y. Ke, G.F. Ren and F.L. Zhu, *Appl. Surf. Sci.*, 476 (2019) 761.
4. Y. Li, J. Wang, J. Yao, H.X. Huang, Z.Q. Du, H Gu and Z.T. Wang, *Mater. Chem. Phys.*, 224 (2019) 293.
5. Y.Q. Chen, K.X. Xiang, W. Zhou, Y.R. Zhu, N.B. Bai and H Chen, *J. Alloy. Compd.*, 749 (2018) 1063.
6. D.S.H. Lee, W.B. Im and X.H. Liang, *Mater. Chem. Phys.*, 232 (2019) 367.
7. L. Bao, G. Xu and M.Y. Wang, *Mater. Charact.*, 157 (2019) 109927.
8. C.S. Zhao, L.N. Wang, H.Wu, J.T. Chen and M. Gao, *Mater. Res. Bull.*, 97 (2018) 195.
9. W.A. Sławiński, H.Y. Playford, S. Hull, S.T. Norberg, S.G. Eriksson, T. Gustafsson, K. Edström and W.R. Brant, *Chem. Mater.*, 31 (2019) 5024.

10. L. Savignac, J.M. Griffin and S.B. Schougaard, *J. Phys. Chem. C.*, 124 (2020) 7608
11. G.D. Du, Y.K. Zhou, X.H. Tian, G. Wu, Y.K. Xi and S.Y. Zhao, *Appl. Surf. Sci.*, 453 (2018) 493.
12. X.F. Wei, Y.B. Guan, X.H. Zheng, Q.Z. Zhu, J.R. Shen, N. Qiao, S.Q. Zhou and B. Xu, *Appl. Surf. Sci.*, 440 (2018) 748.
13. Z.H. Yu and L.H. Jiang, *Solid State Ionics*, 325 (2018) 12.
14. L.P. He, W.K. Zha and D.C. Chen, *Prog. Nat. Sci-Mater.*, 29 (2019) 156.
15. A.A. Adepoju and Q.L. Williams, *Curr. Appl. Phys.*, 20 (2020) 1.
16. P. Rosaiah, J.H. Zhu, O.M.Hussain, Z.G. Liu and Y.J. Qiu, *Electroanal Chem.*, 811 (2018) 1.
17. Y.Y. Wang, X.L. Wang, A. Jiang, G.X. Liu, W.S. Yu, X.T. Dong and J.X. Wang, *J. Alloy. Compd.*, 810 (2019) 151889
18. Y. Liu, Y.J. Gu, G.Y. Luo, Z.L. Chen, F.Z.Wu, X.Y. Dai, Y. Mai and J.Q. Li, *Ceram. Int.*, 46 (2020) 14857.
19. J.K. Ou, L. Yang, F. Jin, S.G. Wu, J.Y. Wang, *Adv. Powder Technol.*, 31 (2020) 1220.
20. D.X. Zhang, J. Wang, K.Z Dong and A.M. Hao, *Comp. Mater. Sci.*, 155 (2018) 410
21. Y.J. Wu, Y.J. Gu, Y.B. Chen, H.Q. Liu and C.Q. Liu, *Int. J. Hydrogen. Energ.*, 43 (2018) 2050
22. S.S Jiang and Y.S Wang, *Solid State Ionics*, 335 (2019) 97.
23. J. Kumar, X. Shen, B. Lia, H.Z. Liu and J.M. Zhao, *Waste Manage.*, 113 (2020) 32.
24. Y. Wang, Z.Y. He, J.J. Chen, K. Liang, K. Marcus and Z.S. Feng, *Mater. Lett.*, 196 (2017) 4.
25. A.K. Budumuru, M. Viji, A. Jen, B.R.K. Nanda and C. Sudakar, *J. Power Sources*, 406 (2018) 50.
26. A. Naik, J. Zhou, C. Gao, G.Z. Liu and L. Wang, *J. Energy Inst.*, 89 (2016) 21.
27. H. Yuan, X.Y. Wang, Q. Wu, H.B. Shu and X.K. Yang, *J. Alloy. Compd.*, 675 (2016) 187.
28. C.Z. Li, H.Y. Yuan and Z.J. Yang, *Solid State Ionics*, 352 (2020) 115366.
29. S. Vedala and M. Sushama, *Mater. Today*, 5 (2018) 1649.
30. A. Eftekhari, *J. Power Sources*, 343 (2017) 395.
31. Y. Liu, M. Zhang, Y. Li, Y.M. Hu, M.Y. Zhu, H.M. Jin and, W.X. Li, *Electrochim. Acta*, 176 (2015) 689.
32. D. Goonetilleke, T. Faulkner, V.K. Peterson and N. Sharma, *J. Power Sources*, 394 (2018) 1.
33. J. Chen, N. Zhao, G.D. Li. F.F. Guo, X.F. Wang, T.K. Jia, J.W. Zhao, Y.G. Zhao and X.L. Wang, *Mater. Chem. Phys.*, 180 (2016) 244.
34. D.W. Xu, X.D. Chu, Y.B. He, Z.J. Ding, B.H. Li, W.J. Han, H.D. Du and F.Y. Kang, *Electrochim. Acta*, 152 (2015) 398.
35. Y.J. Lv, B. Huang, J.X. Tan, S.Q. Jiang, S.F. Zhang and Y.X. Wen, *Mater. Lett.*, 229 (2018) 349.
36. Y. Liu, Y.J. Gu, J.L. Deng, G.Y. Luo, F.Z. Wu, Y. M, X.Y. Dai and J.Q. Li, *J. Mater. Sci-Mater. EL.*, 31 (2020) 2887
37. H.S. Lee, S. Kim, N. S. Parmar, J.H. Song, K.Y. Chung, K.B. Kim and J.W. Choi, *J. Power Sources*, 434 (2019) 226713.